

# PIN-mediated polar auxin transport facilitates root–obstacle avoidance

Hyo-Jun Lee<sup>1,2</sup> , Hyun-Soon Kim<sup>1</sup> , Jeong Mee Park<sup>1,3</sup> , Hye Sun Cho<sup>1,3</sup>  and Jae Heung Jeon<sup>1</sup> 

<sup>1</sup>Plant Systems Engineering Research Center, Korea Research Institute of Bioscience and Biotechnology, Daejeon 34141, Korea; <sup>2</sup>Department of Functional Genomics, KRIBB School of Bioscience, University of Science and Technology, Daejeon 34113, Korea; <sup>3</sup>Department of Biosystems and Bioengineering, KRIBB School of Biotechnology, University of Science and Technology, Daejeon 34113, Korea

Author for correspondence:

Hyo-Jun Lee

Tel: +82 42 860 4497

Email: hyojunlee@kribb.re.kr

Received: 28 May 2019

Accepted: 18 July 2019

*New Phytologist* (2020) **225**: 1285–1296

doi: 10.1111/nph.16076

**Key words:** obstacle avoidance, PIN, polar auxin transport, root bending, thigmotropism.

## Summary

- Plants sense mechanical stimuli to recognise nearby obstacles and change their growth patterns to adapt to the surrounding environment. When roots encounter an obstacle, they rapidly bend away from the impenetrable surface and find the edge of the barrier. However, the molecular mechanisms underlying root–obstacle avoidance are largely unknown.
- Here, we demonstrate that PIN-FORMED (PIN)-mediated polar auxin transport facilitates root bending during obstacle avoidance. We analysed two types of bending after roots touched barriers. In auxin receptor mutants, the rate of root movement during first bending was largely delayed. Gravity-oriented second bending was also disturbed in these mutants.
- The reporter assays showed that asymmetrical auxin responses occurred in the roots during obstacle avoidance. Pharmacological analysis suggested that polar auxin transport mediates local auxin accumulation. We found that PINs are required for auxin-assisted root bending during obstacle avoidance.
- We propose that rapid root movement during obstacle avoidance is not just a passive but an active bending completed through polar auxin transport. Our findings suggest that auxin plays a role in thigmotropism during plant–obstacle interactions.

## Introduction

Due to economic development and industry growth, urban areas have expanded while cropland areas have shrunk in many countries (Cohen, 2006; Long *et al.*, 2007; Lambin & Meyfroidt, 2011). Recent global climate change negatively affects agricultural environments causing reductions of crop yields (Peng *et al.*, 2004; Schlenker & Lobell, 2010; Lobell *et al.*, 2011). However, the rapid increase in global population in the last century demands large amounts of food (Godfray *et al.*, 2010; Tilman *et al.*, 2011). Therefore, it is necessary to grow plants on unfavourable lands with barren, dry or rocky soils. Growth patterns of plants in these areas are different from those in better quality soils. Roots bend away from obstacles and find routes to grow into the deep soils in a process known as obstacle avoidance (Massa & Gilroy, 2003; Tanaka *et al.*, 2010). This tropism helps plants to efficiently anchor themselves and seek nutrients and water to survive harsh conditions.

Plants are able to sense mechanical stimuli like touch to monitor surrounding conditions (Braam, 2005; Jensen *et al.*, 2017). Studies on plant touch responses have expanded since TOUCH-INDUCED (TCH)-coding genes were identified in *Arabidopsis* (Braam & Davis, 1990). The *TCH* genes have highly similar amino acid sequences to calmodulin, suggesting that calcium

(Ca<sup>2+</sup>) signalling is involved in touch responses. Following this discovery, research focused on the ion channels and membrane proteins that control Ca<sup>2+</sup> flux in order to uncover touch-related mechanosensory pathways. Plasma membrane-localised MID1-COMPLEMENTING ACTIVITY 1 (MCA1) promotes Ca<sup>2+</sup> influx into the cytoplasm upon mechanical stimulation (Nakagawa *et al.*, 2007). Overexpression of *MCA1* disturbs growth and causes constitutive expression of the *TCH3* gene. *MCA1*-defective mutants show defective penetration of hard agar, suggesting that *MCA1*-mediated Ca<sup>2+</sup> flux is involved in touch responses of roots.

Ca<sup>2+</sup> flux is also closely related to root bending. Cytosolic Ca<sup>2+</sup> concentration rapidly increases on the convex side of epidermal cells upon bending (Monshausen *et al.*, 2009). Transiently increased Ca<sup>2+</sup> triggers the production of apoplastic reactive oxygen species (ROS) and cytoplasmic acidification, which are involved in cell growth. These reports suggest that bending causes asymmetrical touch-like responses in roots. Recent studies have shown that bending-induced Ca<sup>2+</sup> responses are regulated by FERONIA (FER) receptor-like kinase (Shih *et al.*, 2014). *FER*-deficient mutants alter expression of *TCH* genes and root bending angle during obstacle avoidance, implying that *FER*-mediated Ca<sup>2+</sup> signalling is important for asymmetrical cell elongation in roots. In addition to Ca<sup>2+</sup> responses, asymmetrical extracellular ATP responses are also observed in roots upon touch

(Weerasinghe *et al.*, 2009). However, the role of these distinct responses during root bending or touching remains largely unknown.

Tropism of plant bodies is linked to asymmetrical auxin distribution caused by polar auxin transport (Friml *et al.*, 2002; Ottenschläger *et al.*, 2003; Lewis *et al.*, 2007). In *Arabidopsis*, auxin transporters have been identified as important players in polarised auxin responses. PIN-FORMED (PIN) proteins are auxin-efflux carriers, and their roles and functions have been studied extensively. In many cases, PINs mediate root tropism and the root is highly sensitive to environmental cues. Root gravitropism is controlled by proteasome-mediated asymmetrical degradation of PIN2 in the root cells (Abas *et al.*, 2006). PIN2 also regulates root halotropism and negative phototropism (Wan *et al.*, 2012; Galván-Ampudia *et al.*, 2013). In PIN2-deficient mutants, roots cannot rapidly bend away from areas of high salt or blue light. Intracellular trafficking of PIN2 is triggered by external signals, generating asymmetrical auxin accumulation and cell elongation (Wan *et al.*, 2012; Galván-Ampudia *et al.*, 2013).

In this study, we demonstrated that root bending is accelerated by auxin action during obstacle avoidance. When roots touched a barrier, auxin accumulated on the concave side of the roots. PIN-mediated polar auxin transport promoted asymmetrical auxin accumulation, which leads to rapid root bending away from the barrier. A few hours after first bending, roots underwent a second bending toward a gravity vector. Our work shows that roots actively control their growth rate to rapidly avoid obstacles, and that polar auxin transport is involved in the thigmotropic responses of roots during obstacle avoidance.

## Materials and Methods

### Plant materials and growth conditions

*Arabidopsis thaliana* seedlings were used in this study. The *pin1-5* (CS69067), *eir1-1* (CS8058), *eir1-4* (CS859601), *pin4-3* (CS9368), *pin5-3* (SALK-021738), *pin6* (SALK-095142), *pin7-3* (CS9367), *pin8* (SALK-044651), and *DR5rev:GFP* (CS9361) seeds were obtained from the Arabidopsis Biological Resource Center (ABRC, Ohio State University, Columbus, OH, USA). The *tir1-1* (N3798), *pin3-4* (N9363), *fer-4* (N69044), *aux1-7* (N9583), and *DII-VENUS* (N799173) seeds were obtained from the Nottingham Arabidopsis Stock Centre (NASC, Nottingham, UK). The *tir1-1 afb1-1 afb2-1 afb3-1* quadruple mutant (Dharmasiri *et al.*, 2005b) and *pin3-3 pin4-3 pin7-1* triple mutant (Waldie & Leyser, 2018) seeds were described previously.

Seeds surface-disinfected using 70% ethanol were incubated at 4°C for 3 d and then transferred to a growth room set at 24°C and at c. 50% humidity. Seedlings were grown on half-strength Murashige and Skoog agar (½MS agar) plates under long days (LDs; 16 h : 8 h, light : dark cycles). White light with an intensity of 100 µmol m<sup>-2</sup> s<sup>-1</sup> was applied using fluorescent FL40EX-D tubes (Focus, Bucheon, Korea).

### Measurement of root bending angles

For obstacle avoidance, seedlings were grown on vertically oriented MS agar plates (1% agar) for 5 d. Corrosion-resistant BA-400 blades (CUTTERMALLKOREA, Seoul, Korea) were used as obstacles. Obstacles were installed vertically on the MS agar plates and 5-d-old seedlings were laid 2 mm above the obstacles. Root growth and movement were photographed every 20 min. To measure rate of first bending, the angle between the roots was measured at 0 min and at annotated time points after contact with the barrier using IMAGEJ software (<https://imagej.nih.gov/ij/>). For the second bending, the angles between the root tips and the barrier were measured 200 min after the roots touched the obstacle.

### Confocal microscopy

Here, 5-d-old *DR5rev:GFP* or *DII-VENUS* seedlings were transferred to obstacle-installed MS agar plates. Fluorescence during first and second bending was observed 20–40 min and 150–200 min after the roots touched obstacles, respectively. To visualise root cells, roots were immersed in 10 µM propidium iodide (PI) solution for 30 s before observing fluorescence. Seedlings were placed on slide glasses and were subjected to fluorescence imaging using an LSM 800 confocal microscope (Carl Zeiss, Oberkochen, Germany). Fluorescence images were analysed using ZEN 2.5 LITE software (<https://www.zeiss.com>).

For quantification of fluorescence intensities, we used IMAGEJ software. When using *DR5rev:GFP* reporter plants, GFP fluorescence intensities at the later root cap cells, which are located at 100–200 µm from the root tip were analysed to quantify lateral auxin distributions. PI fluorescence intensities at the same region were also quantified as controls.

### Pharmacological treatment

For *N*-1-naphthylphthalamic acid (NPA; Sigma-Aldrich, St Louis, MO, USA, cat. no. 33371), 5-(4-chlorophenyl)-4H-1,2,4-triazole-3-thiol (yucasin; Carbosynth, Berkshire, UK; cat. no. FC122238), and L-kynurenine (L-Kyn; Sigma-Aldrich; cat. no. K8625) treatments, 5-d-old seedlings grown on MS agar plates were transferred to the obstacle-installed plates containing 25 µM NPA, 50 µM yucasin, or 1 µM L-Kyn. The roots grew for c. 5 h in the medium before making contact with the obstacle. For ethylene glycol tetraacetic acid (EGTA) treatment, 5-d-old seedlings were transferred to 2 mM EGTA-containing plates before measuring obstacle avoidance. As up to 10 mM EGTA is used to block Ca<sup>2+</sup> signalling in *Arabidopsis* (Zhang & Mou, 2009; Ma *et al.*, 2017), we applied 2 mM EGTA in this article.

### Statistical analysis

The statistical significance between two means of measurements was analysed using Student's *t*-test with the *P*-value < 0.05. Numbers of replications are annotated in the figure legends.

Quantitative data are displayed as standard deviations of the mean (SD).

## Results

### Roots rapidly bend away from the obstacle after contact with barrier

Roots exhibit step-like growth patterns when they sense obstacles (Massa & Gilroy, 2003). First bending occurs in the root apex transition zone, which is located at *c.* 700  $\mu\text{m}$  from the root tip (Massa & Gilroy, 2003). Second bending starts a few hours after contact with the barrier in the root apex that lies *c.* 410  $\mu\text{m}$  from the tip. Most studies on root–obstacle avoidance focus on the second bending because it is thought that the first bending is simply passive due to root growth against a barrier (Shih *et al.*, 2014). However, asymmetrical  $\text{Ca}^{2+}$  and ATP responses in root cells after the root tip touches a barrier suggest that active signal transduction is involved in the first bending during obstacle avoidance (Monshausen *et al.*, 2009; Weerasinghe *et al.*, 2009).

To evaluate whether the first bending is a passive or an active bending, we systemically analysed the movement of roots during obstacle avoidance. Col-0 seedlings were arranged vertically against a barrier and were photographed every 20 min. As reported in previous studies, roots exhibited two-step bending during interactions with barriers (Fig. 1a). First bending occurred 20–80 min after the roots touched the barrier, and second bending started to occur *c.* 120 min after contact. After second bending, roots maintained step-like forms and grew parallel to the barrier until meeting the edge of the obstacle.

We then carefully monitored root movement during first bending. Roots showed rapid and sharp bending after touching the barrier. The upper part of the bending region did not move during the first bending, while the lower part including root tip bent away from the barrier (Fig. 1b). To analyse the rate of first bending, we measured the bending angles between the roots at 0 min and every 20 min after contact with the barrier (Fig. 1c, left panel). We found that bending rate was highest during the first 20 min, while it was relatively constant 20–80 min after contact (Fig. 1c, right panel).

Based on our observations of root bending during the initial phase of obstacle avoidance, we hypothesised that asymmetrical cell elongation occurs during the first bending. When roots meet barriers, they may transmit asymmetrical signals to trigger local activation of cell elongation. The asymmetrical cell growth would confer sharp and high-rate bending during obstacle avoidance (Fig. 1d).

### Auxin controls root bending during obstacle avoidance

Auxin is involved in diverse plant tropisms including halotropism, phototropism, and gravitropism (Abas *et al.*, 2006; Wan *et al.*, 2012; Galván-Ampudia *et al.*, 2013). We therefore hypothesised that auxin might play a role in thigmotropism of roots during obstacle avoidance. To investigate the role of auxin, we observed the bending patterns of TRANSPORT INHIBITOR RESPONSE 1/AUXIN SIGNALLING F BOX PROTEIN (TIR1/AFB)-deficient mutants because TIR1/AFB auxin receptors play a critical role in auxin-controlled cell elongation (Dharmasiri *et al.*, 2005a; Fendrych *et al.*, 2016). We used

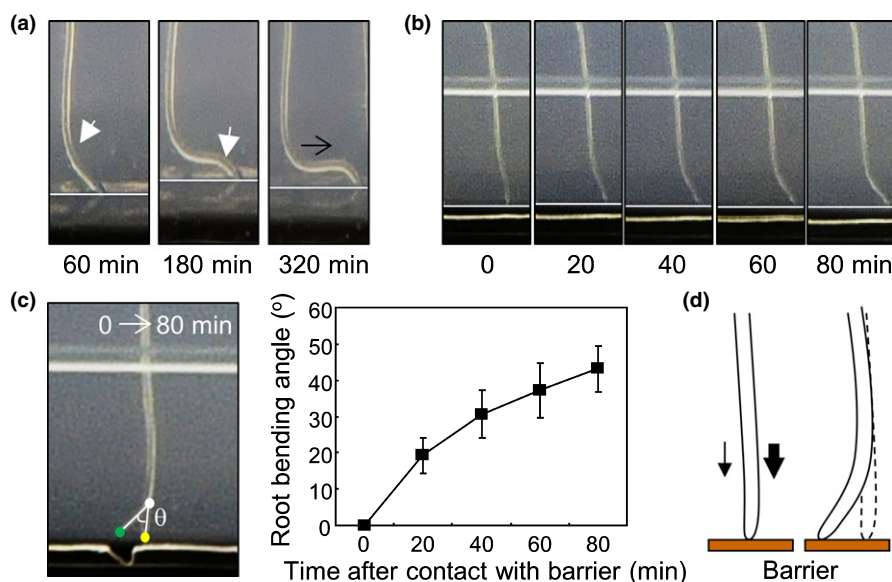


**Fig. 1** Arabidopsis roots exhibit rapid tropic responses during obstacle avoidance. (a) Three phases of root–obstacle avoidance. Col-0 seedlings grown on MS agar plates for 5 d under long days (LDs) were laid 2 mm above the obstacle. Root movement was photographed in a time-course manner. Roots touched the barrier at 0 min. White arrows indicate the bending point of roots. Black arrow indicates growth of roots parallel to the barrier. (b, c) Movement of roots during the first bending. Here, 5-d-old Col-0 seedlings were treated as described in (a) were photographed every 20 min (b). Angles between the roots at 0 min and the roots at indicated time points were set to  $\theta$  (c, left panel). Seven replicates at each time point were averaged (c, right panel). Whiskers indicate  $\pm$  SD. (d) Hypothesis on the first bending of the roots during obstacle avoidance. Asymmetrical growth hypothesis during the first bending was illustrated.



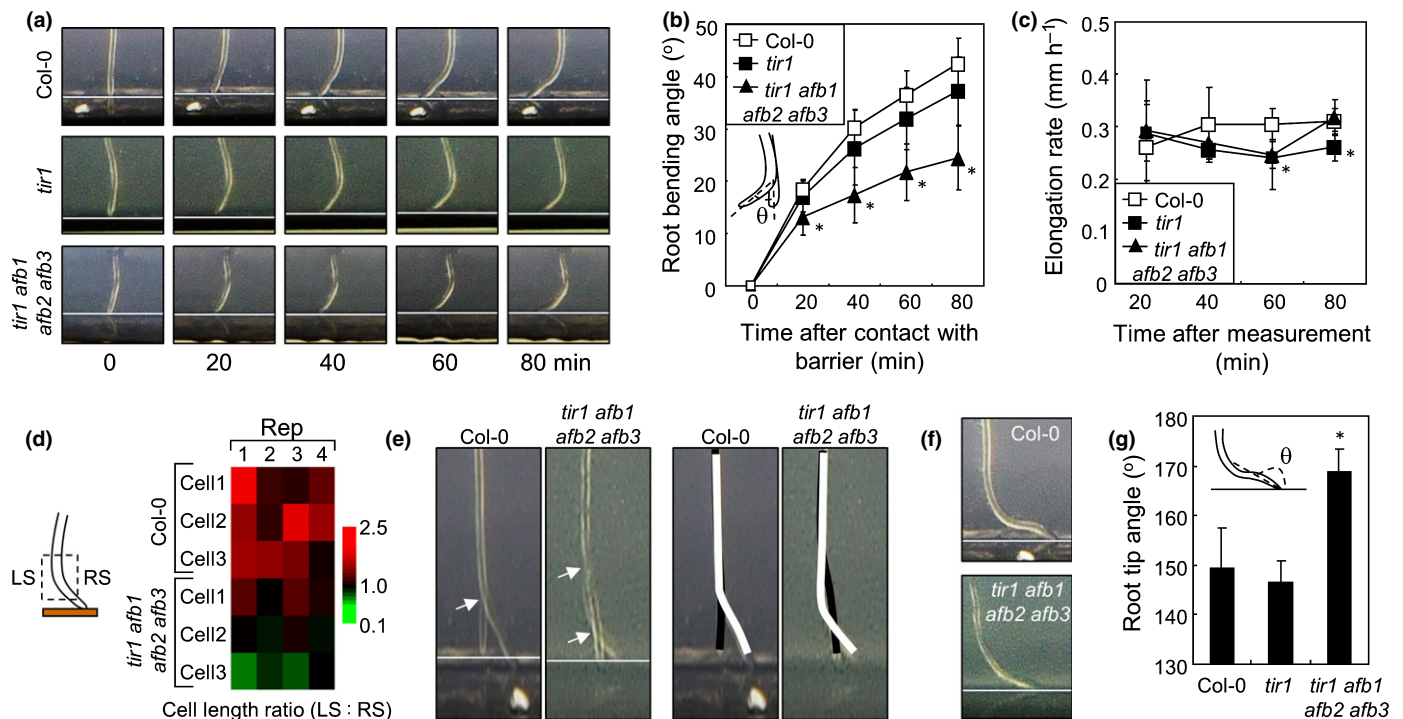


**Fig. 2** Auxin receptors are involved in root–obstacle avoidance. Here, 5-d-old Arabidopsis seedlings grown on MS agar plates were used for the assays. Note that *tir1* and *tir1 afb1 afb2 afb3* indicate *tir1-1* and *tir1-1 afb1-1 afb2-1 afb3-1* quadruple mutants, respectively. (a, b) Effects of auxin receptor gene mutations on the first bending during obstacle avoidance. Root bending angles of *tir1* and quadruple *tir1 afb1 afb2 afb3* mutants were photographed every 20 min after contact with barrier (a). Bending angles of roots were measured as described in Fig. 1(c). (b). Eight replicates were averaged and statistically analysed using Student's *t*-test (\*,  $P < 0.01$ ). Whiskers indicate  $\pm$ SD. (c) Root growth rate of auxin receptor mutants. Root elongation rate was measured before contact with the barrier. Eight replicates were averaged. Whiskers indicate  $\pm$ SD. (d) Cell length ratio in *tir1 afb1 afb2 afb3* quadruple mutants during the first bending. Epidermis cell lengths of Col-0 and quadruple *tir1 afb1 afb2 afb3* roots were measured as described in Supporting Information Fig. S2 using IMAGEJ software. Cell lengths at LS were divided by those at RS to calculate cell length ratio. Cell length ratios were visualised using heatmap. Heatmap bar, cell length ratio ( $\log_2$  value). (e) Different root bending patterns between Col-0 and auxin receptor mutants. Photographs at 0 min and 80 min were overlapped. White arrows indicate the point of contact between the roots at 0 min and at 80 min (left panel). The black line shows roots at 0 min and the white line shows roots at 80 min (right panel). Note that gradual bending of quadruple *tir1 afb1 afb2 afb3* mutants exhibited different bending pattern than Col-0 roots. (f, g) Effects of auxin receptor gene mutations on the second bending during obstacle avoidance. Roots were photographed 200 min after contact with the barrier (f). The angles between the root tip and the barrier were set to  $\theta$  (g). Eight replicates were averaged and statistically analysed using Student's *t*-test (\*,  $P < 0.01$ ). Whiskers indicate  $\pm$ SD.

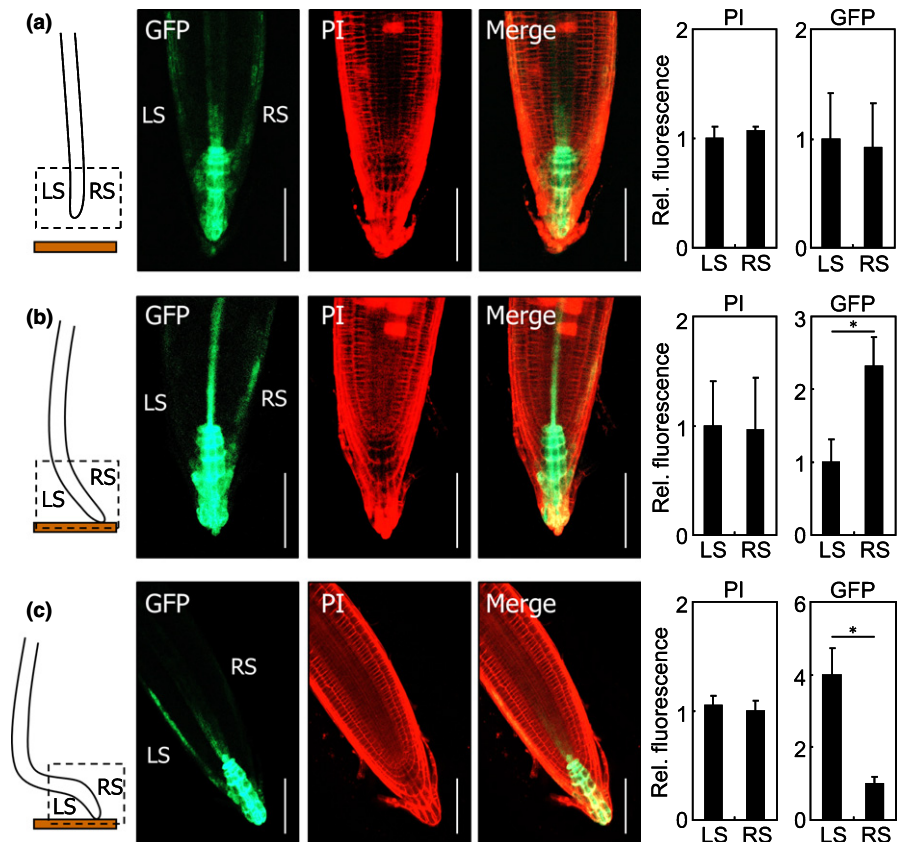
*tir1-1* and quadruple *tir1-1 afb1-1 afb2-1 afb3-1* mutants. As quadruple *tir1 afb1 afb2 afb3* mutants exhibited multiple classes in root phenotypes (Supporting Information Fig. S1; Dharmasiri *et al.*, 2005b), we selected the class III that root length of the quadruple *tir1 afb1 afb2 afb3* mutants was similar to that of Col-0 to compare root–obstacle avoidance. In our experiment, rates of first bending in Col-0 and *tir1* roots were indistinguishable, while bending rate of quadruple *tir1 afb1 afb2 afb3* roots was significantly reduced compared with Col-0 roots (Fig. 2a,b). We also measured rate of root elongation before the roots touched the barrier, because reduced bending rate might be due to defects in root growth. Roots of both *tir1* and quadruple *tir1 afb1 afb2 afb3* mutants showed similar prebarrier growth rates to Col-0 roots, while quadruple *tir1 afb1 afb2 afb3* mutants showed a reduced growth rate at several time points (Fig. 2c). To examine whether the defective first bending in quadruple *tir1 afb1 afb2 afb3* mutants is due to impaired asymmetrical cell elongation in the bending region, we measured root epidermis cell length after the first bending. We defined that the left side (LS) is the convex side and the right side (RS) is the concave side during the first

bending. Cell lengths at LS were divided by those at the opposite side (RS) to calculate cell length ratio (Fig. S2). Cell length ratios in Col-0 roots were consistently higher than 1.0, but those in quadruple *tir1 afb1 afb2 afb3* roots showed a high variation (Fig. 2d). These results suggested that auxin perception is important for rapid bending and asymmetrical cell elongation during the initial phase of obstacle avoidance.

To examine why quadruple *tir1 afb1 afb2 afb3* mutants exhibited a reduced bending rate, we observed the growth pattern of the roots during the first bending. While Col-0 roots bent sharply in the root apex transition zone, quadruple *tir1 afb1 afb2 afb3* roots bent gradually, generating two points of contact between the roots at 0 min and at 80 min (Fig. 2e). Therefore, it is possible that gradual root bending due to the lack of auxin action and asymmetrical cell elongation is the reason for decreased bending rate in quadruple *tir1 afb1 afb2 afb3* mutants.

We also analysed the second bending of *tir1* and quadruple *tir1 afb1 afb2 afb3* roots during obstacle avoidance. The angle between root tip and the barrier was measured following the methodology of previous studies on root–obstacle avoidance

**Fig. 3** Asymmetrical auxin responses in the roots during obstacle avoidance. Here, 5-d-old *DR5rev:GFP* Arabidopsis seedlings grown on MS agar plates were used for the assays. Fluorescence intensities were quantified using IMAGEJ software. Four replicates were averaged and statistically analysed using Student's *t*-test (\*,  $P < 0.01$ ). Whiskers indicate  $\pm$ SD. Bars, 100  $\mu$ m. LS and RS indicate left and right side of the roots, respectively. (a) Auxin responses in the roots before contact with barrier. Seedlings were laid 2 mm above the barrier (left panel). GFP fluorescence in the root tip was observed (middle panel). To visualise root cells, roots were stained in 10  $\mu$ M PI solution. Fluorescence intensities in lateral root cap cells were measured (right panel). Fluorescence intensities at LS were set to 1. LS and RS indicate left and right sides of the roots, respectively. (b) Auxin responses in the roots during the first bending. Seedlings were treated as described in (a). GFP fluorescence was observed 20–40 min after contact with the barrier. Fluorescence intensities at LS were set to 1. (c) Auxin responses in the roots during the second bending. Seedlings were treated as described in (a). GFP fluorescence was observed 150–200 min after contact with barrier. Fluorescence intensities at RS were set to 1.



(Massa & Gilroy, 2003; Shih *et al.*, 2014). Roots of Col-0 and *tir1* seedlings showed similar bending patterns, but the angles of quadruple *tir1 afb1 afb2 afb3* roots were significantly different from those of Col-0 roots (Fig. 2f,g). Together with the observations on first bending, these results indicated that TIR1/AFB-mediated auxin perception is required for thigmotropic movement of roots during obstacle avoidance.

### Asymmetrical auxin responses occur in roots during obstacle avoidance

Local auxin accumulation drives root and shoot tropisms in response to various environmental signals (Friml *et al.*, 2002; Ottenschl ger *et al.*, 2003; Lewis *et al.*, 2007; Ding *et al.*, 2011). We therefore investigated auxin responses in the roots during obstacle avoidance. To visualise auxin responses, we utilised the *DR5rev:GFP* reporter, which is broadly used to study auxin-responsive transcription in plant cells (Ottenschl ger *et al.*, 2003; Blilou *et al.*, 2005). To visualise root cells and to determine location of auxin responses, we stained Col-0 roots with PI solution.

First, we observed GFP and PI fluorescence before the roots touched the barrier as a control. Root tips were targeted for the assays as the *DR5rev:GFP* reporter showed auxin maxima in this region (Sabatini *et al.*, 1999; Ottenschl ger *et al.*, 2003). High intensity GFP fluorescence was detected in the quiescent centre and columella cells as reported previously (Ottenschl ger *et al.*, 2003), while low intensity GFP fluorescence was observed in other parts of the roots (Fig. 3a). During first bending, different

patterns of GFP fluorescence were observed. High intensity GFP fluorescence was detected in the lateral root cap cells on the concave side (RS) of the roots, while it remained at low intensity on the convex side (LS) of the roots (Fig. 3b).

We next observed GFP fluorescence after the roots started the second bending. Again, high intensity GFP fluorescence was detected on the concave side of the roots (Fig. 3c). As local auxin accumulation inhibits cell elongation in the roots (Ottenschl ger *et al.*, 2003; Swarup *et al.*, 2007), auxin responses on the concave side are consistent with the tropic movement of the roots during the obstacle avoidance. The local auxin responses were confirmed using *DII-VENUS* seedlings. Auxin accumulation reduces *DII-VENUS* fluorescence (Brunoud *et al.*, 2012). Similar to the results of the *DR5rev:GFP* assays, high auxin responses were detected on the concave side of the roots during first and second bendings (Fig. S3). These results indicate that root–obstacle interaction triggers asymmetrical auxin responses in the roots.

### Root–obstacle avoidance is regulated by polar auxin transport

In many cases, asymmetrical auxin responses are mediated by polarised auxin transport (Abas *et al.*, 2006; Wan *et al.*, 2012; Galv n-Ampudia *et al.*, 2013). To examine whether polar auxin transport is involved in obstacle avoidance by the roots, we applied NPA, yucasin and L-Kyn. NPA is an auxin transporter inhibitor. Yucasin and L-Kyn are auxin biosynthesis inhibitors that suppress YUCCA and TRYPTOPHAN

AMINOTRANSFERASE OF ARABIDOPSIS1/ TRYPTOPHAN AMINOTRANSFERASE RELATEDs (TAA1/TARs)-mediated auxin biosynthesis, respectively (He *et al.*, 2011; Nishimura *et al.*, 2014). We transferred Col-0 seedlings grown on MS agar plates to the NPA, yucasin- or L-Kyn-containing plates and allowed these to grow until they interacted with obstacles. We used this method to block possible touch-induced auxin transport or biosynthesis. During the first bending, NPA-treated roots exhibited a reduced rate of bending while the yucasin and L-Kyn-treated roots did not show any differences when compared with the control treatment (Figs 4a, S4a). Yucasin did not change root elongation rate, but NPA and L-Kyn affected root elongation rate at several time points (Figs 4b, S4b). As only NPA caused defects in the first bending, we observed cell length of NPA-treated roots during the first bending. Most of the cell length ratios (LS/RS) in mock-treated roots showed higher than 1.0 (Fig. 4c). However, cell length ratios in NPA-treated roots exhibited high variation near 1.0 (Fig. 4c), suggesting that NPA inhibits asymmetrical cell elongation during the first bending. We next observed the effects of NPA, yucasin and L-Kyn on the second bending. Bending of root tips towards the gravity vector was largely disturbed in NPA and L-Kyn-treated roots, while bending was indistinguishable between control and yucasin-treated roots (Figs 4d, S4c). These results indicated that auxin transport is a major factor in the first bending, while both auxin transport and biosynthesis are involved in the second bending during obstacle avoidance.

Next, we analysed the effects of NPA on auxin responses in the roots. We used mock- and yucasin-treated roots as controls because both treatments did not cause any changes in obstacle avoidance. In the NPA treatment, asymmetrical auxin responses on the concave side (LS) of the roots disappeared (Fig. 4e). Likewise, polarised auxin responses during the second bending were not detected in the NPA-treated roots (Fig. 4f). These results indicated that auxin transport-mediated asymmetrical auxin responses are necessary for both the first and second bendings in the roots during obstacle avoidance.

### PINs mediate obstacle avoidance of roots

In Arabidopsis, auxin-efflux carrier PINs mediate polar auxin transport in response to unilateral light or gravity (Abas *et al.*, 2006; Ding *et al.*, 2011; Wan *et al.*, 2012). As our data suggested that polar auxin transport is involved in root movement during obstacle avoidance, we investigated the role of PINs during thigmotropic responses. We first measured the rate of the first bending in PIN-deficient mutants. In this study, PIN1- and PIN7-deficient mutants were on the *Ler* background, while the other *pin* mutants were on the Col-0 background. We found that only PIN2-deficient *eir1-4* roots exhibited largely delayed root movement after contact with barriers (Fig. 5a). The elongation rate of *eir1-4* roots was slightly reduced (Fig. 5b). However, it appears that slow root elongation in *eir1-4* mutants was not the main reason for delayed bending, because Col-0 and *pin4* roots showed similar bending rates even though root elongation rate was significantly decreased in *pin4* roots (Fig. 5a,b). Disturbed first

bending and reduced root elongation rate were also observed for another allele of *pin2* mutants, *eir1-1* (Fig. S5a,b). Cell length ratios between LS and RS in *eir1-4* roots were highly variable near 1.0, while those in Col-0 roots showed consistently as > 1.0 (Fig. 5c). Similar results were also observed in *eir1-1* roots (Fig. S5c). These results suggested that PIN2 controls the first bending during obstacle avoidance.

We next measured the angles between root tips and barriers in *pin* mutants during the second bending. In this assay, *eir1-4* and *pin3* mutants exhibited altered bending responses, while bending angles of the other mutants were not significantly different to those of Col-0 (Fig. 5d). The second bending of *eir1-1* roots was also significantly disturbed (Fig. S5d). As PIN2 and PIN3 functions are important in root gravitropism (Abas *et al.*, 2006; Rakusová *et al.*, 2011), it is unsurprising that *pin2* and *pin3* mutants were impaired in the second bending because the second bending is largely affected by gravitropic responses (Massa & Gilroy, 2003).

To verify the role of PIN2 in root–obstacle avoidance, we crossed *DR5rev:GFP* transgenic plants with *eir1-1* mutants to analyse auxin response patterns in the roots. During the first bending, local auxin responses were detected in Col-0 background roots, as shown in Figs 3, 4 (Fig. 5e). However, asymmetrical auxin responses in the roots were prevented by the *eir1-1* mutation. Similar patterns were observed during the second bending. Polarised auxin responses in the Col-0 roots were largely impaired in *eir1-1* mutants (Fig. 5f), suggesting that PIN2 plays a key role in polar auxin transport-mediated root movement during obstacle avoidance.

PIN3, -4 and -7 have functional redundancy, therefore auxin transport-defective phenotypes are usually observed in *pin3 pin4 pin7* triple mutants (Blilou *et al.*, 2005). We therefore analysed root–obstacle avoidance in *pin3-3 pin4-3 pin7-1* triple mutants. Like *pin2* mutants, *pin3 pin4 pin7* triple mutants had defects in the first bending and root elongation rate (Fig. S6a,b). Measuring cell length ratio in *pin3 pin4 pin7* triple mutants showed that asymmetrical cell elongation was also impaired by *pin3 pin4 pin7* triple mutations (Fig. S6c). In addition, *pin3 pin4 pin7* triple mutants exhibited defective second bending (Fig. S6d). However, another auxin transporter mutant *aux1-7* only showed altered second bending (Fig. S7), suggesting that PINs are major players in the first bending during obstacle avoidance.

### Ca<sup>2+</sup> signalling is involved in root–obstacle avoidance

During root–obstacle interactions, cytosolic Ca<sup>2+</sup> concentration is increased on the convex side of the roots (Monshausen *et al.*, 2009). However, it remains unknown whether the transient increase in Ca<sup>2+</sup> level affects root growth during obstacle avoidance. To examine the relationship between Ca<sup>2+</sup> and root bending, we treated roots with a Ca<sup>2+</sup> chelator, EGTA. During first bending, EGTA-treated roots showed a delayed bending rate and reduced root growth (Fig. 6a,b). Asymmetrical cell elongation during the first bending was largely suppressed by EGTA treatment (Fig. 6c). EGTA also negatively affected the second bending of the roots (Fig. 6d). As EGTA treatment impairs root



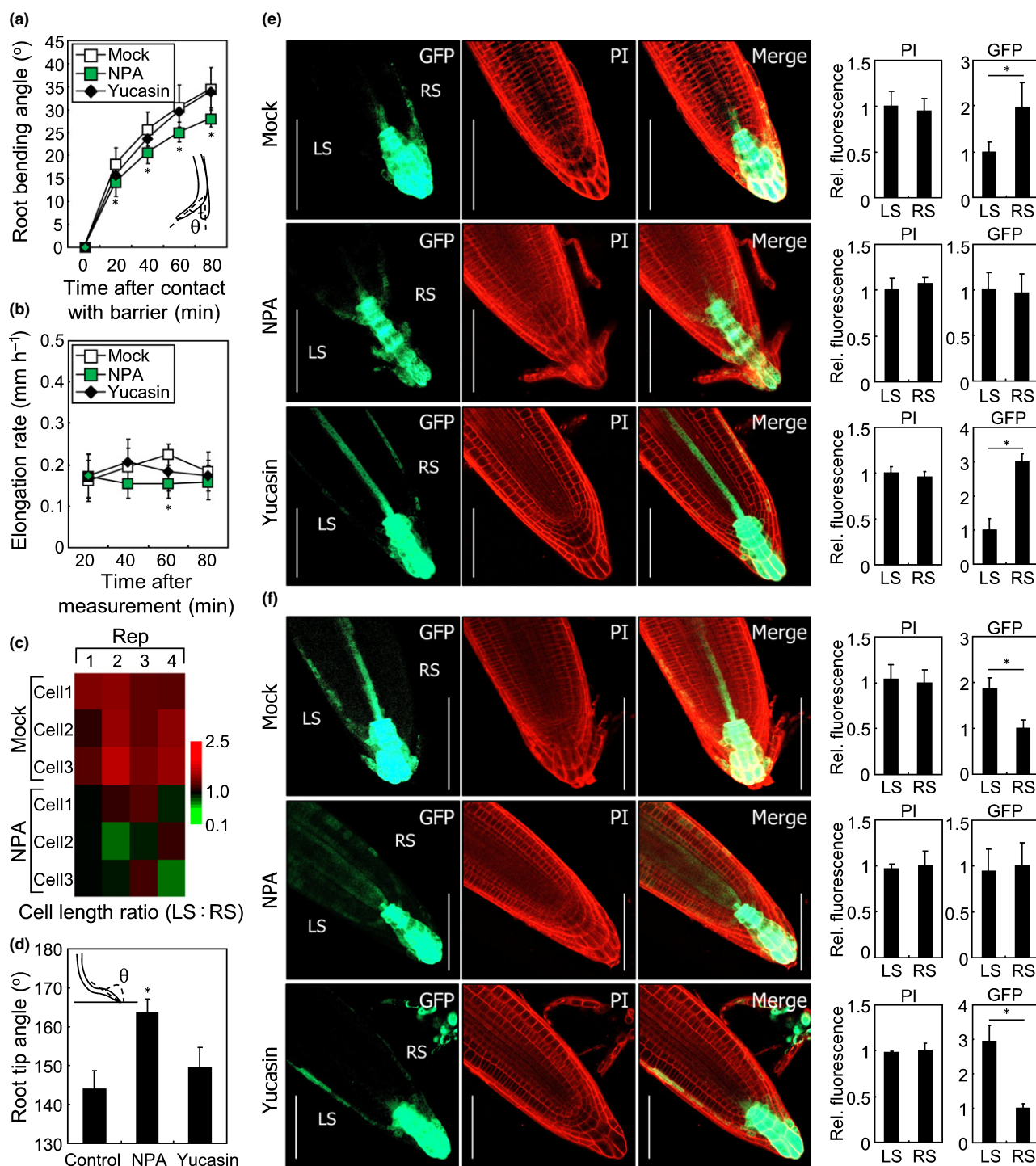


**Fig. 4** Polar auxin transport facilitates root obstacle avoidance. Here, 5-d-old *Arabidopsis* seedlings grown on MS agar plates were used for the assays. Replicates were statistically analysed using Student's *t*-test (\*,  $P < 0.05$ ). Whiskers, SD. LS and RS indicate left and right side of the roots, respectively. (a) Effects of NPA and yucasin on the first bending during obstacle avoidance. Seedlings were transferred to MS agar plates containing 25  $\mu$ M NPA or 50  $\mu$ M yucasin. The roots grew for c. 5 h before they touched the obstacle. Bending angles of the roots were measured as described in Fig. 1(c). Eight replicates were averaged. (b) Effects of NPA and yucasin on root elongation rate. Seedlings were treated as described in (a). Root elongation rate was measured before contact with barrier. Eight replicates were averaged. (c) Cell length ratio in NPA-treated roots during the first bending. NPA was applied to Col-0 seedlings as described in (a). Cell length ratio was calculated as described in Fig. 2(d). Heatmap bar, cell length ratio ( $\log_2$  value). (d) Effects of NPA and yucasin on the second bending during obstacle avoidance. Seedlings were treated as described in (a). Bending angles of the roots were measured as described in Fig. 2(g). Eight replicates were averaged. (e, f) Effects of NPA and yucasin on auxin responses during obstacle avoidance. *DR5rev::GFP* seedlings were used for the assays. The NPA and yucasin were applied to Col-0 seedlings as described in (a). GFP and PI fluorescence during the first bending (e) and the second bending (f) were observed as described in Fig. 3(b,c), respectively. Bars, 100  $\mu$ m. Fluorescence intensities were measured using IMAGEJ software. Four replicates were averaged.

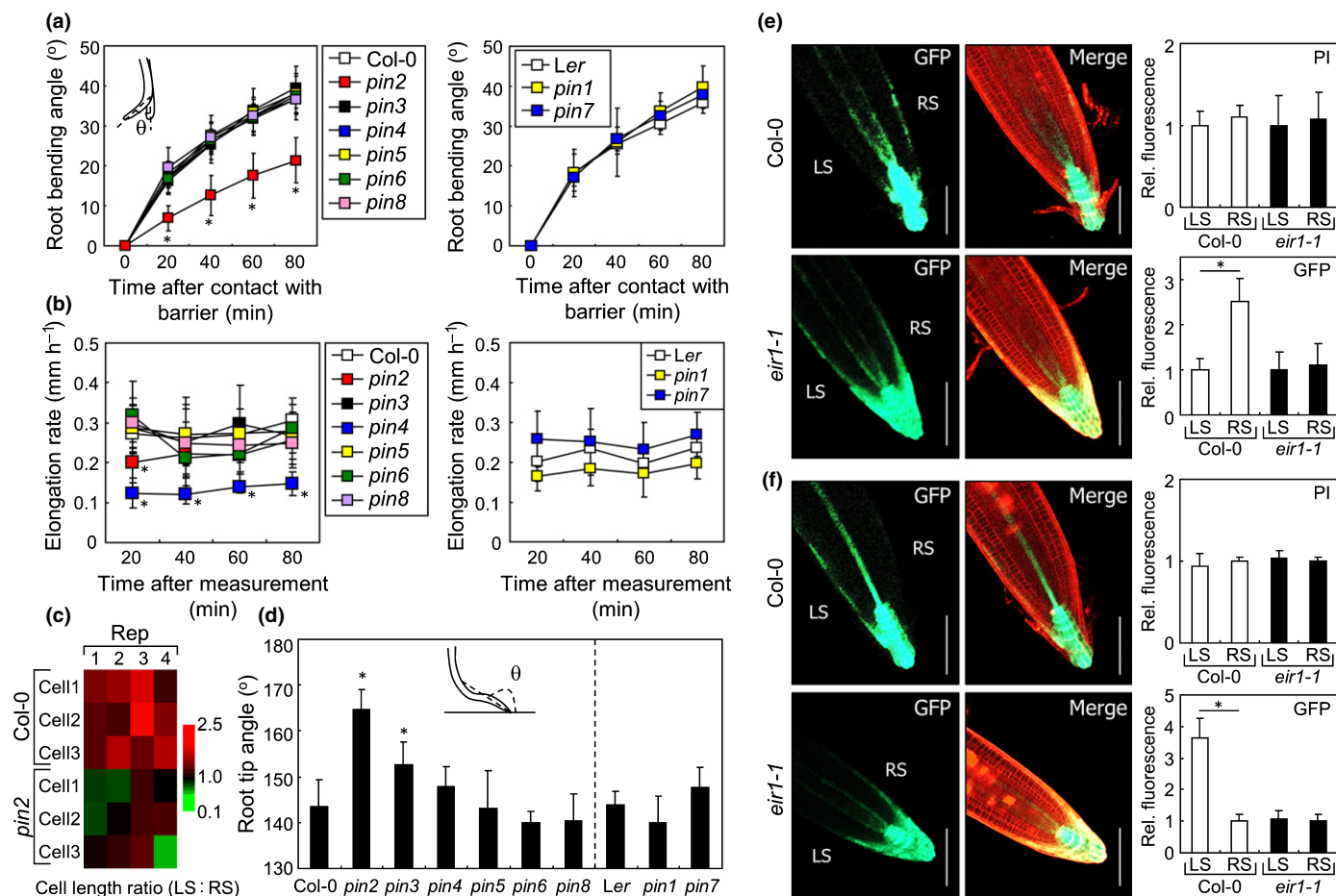


**Fig. 5** PINs control polar auxin transport during root–obstacle avoidance. Here, 5-d-old Arabidopsis seedlings grown on MS agar plates were used for the assays. Replicates were statistically analysed using Student's *t*-test (\*,  $P < 0.05$ ). Whiskers,  $\pm$ SD. LS and RS indicate left and right side of the roots, respectively. (a) First bending of *pin* roots during obstacle avoidance. Bending angles of the roots were measured as described in Fig. 1(c). Eight replicates were averaged. Note that *pin2* indicates *eir1-4*. (b) Root elongation rate of *pin* mutants. Root elongation rate was measured before contact with barrier. Eight replicates were averaged. (c) Cell length ratio in *pin2* roots during the first bending. Root epidermis cell lengths were measured as described in Fig. 2(d). Heatmap bar, cell length ratio (log<sub>2</sub> value). (d) Second bending of *pin* roots during obstacle avoidance. Bending angles of the roots were measured as described in Fig. 2(g). Eight replicates were averaged. (e, f) Auxin responses in *eir1-1* roots. *DR5rev:GFP* and *DR5rev:GFP*  $\times$  *eir1-1* seedlings were used for the assays. GFP and PI fluorescence during the first bending (e) and the second bending (f) were measured as described in Fig. 3(b,c), respectively. Bars, 100  $\mu$ m. Fluorescence intensities were measured using IMAGEJ software. Four replicates were averaged.

gravitropism (Sinclair & Trewavas, 1997; Takahashi *et al.*, 2009), it seems that a disturbed second bending in EGTA-treated roots is due to a malfunction in the gravitropic responses.

To investigate whether EGTA affects auxin transport, we treated *DR5rev:GFP* reporter plants with EGTA and analysed GFP fluorescence during obstacle avoidance. We found that EGTA inhibited asymmetrical auxin responses in the roots during both the first and second bendings (Fig. 6e,f), suggesting that  $\text{Ca}^{2+}$  signalling is important for polar auxin transport during root–obstacle interactions. However, we could not find any clues on the relationship between  $\text{Ca}^{2+}$  and PIN-mediated auxin transport. As EGTA treatment did not change *PIN2* gene expression during the first bending (Fig. S8), it is possible that  $\text{Ca}^{2+}$  affects PIN protein dynamics during obstacle avoidance.

A transient and biphasic  $\text{Ca}^{2+}$  increase is observed in the epidermis on the convex side of the bent root (Shih *et al.*, 2014). The receptor-like kinase FER mediates the second peak of the  $\text{Ca}^{2+}$  response, therefore a monophasic  $\text{Ca}^{2+}$  peak is observed in

FER-deficient mutants (Shih *et al.*, 2014). To investigate whether the FER-mediated  $\text{Ca}^{2+}$  response is involved in root–obstacle avoidance, we measured bending angles of *fer-4* mutants after contact with a barrier. We found that bending rate of *fer-4* roots during first bending was similar to that of the Col-0 roots (Fig. 6g,h), while *fer-4* mutants showed an impaired second bending as reported previously (Fig. 6i; Shih *et al.*, 2014). These results suggested that FER-mediated  $\text{Ca}^{2+}$  response is only involved in the second bending during obstacle avoidance.

## Discussion

### The role of auxin during root–obstacle avoidance

In this work, we demonstrated that roots recognise obstacles and actively avoid them using asymmetrical auxin accumulation. When roots touched an obstacle, PIN-mediated polar auxin transport was activated to accumulate auxin on the concave side



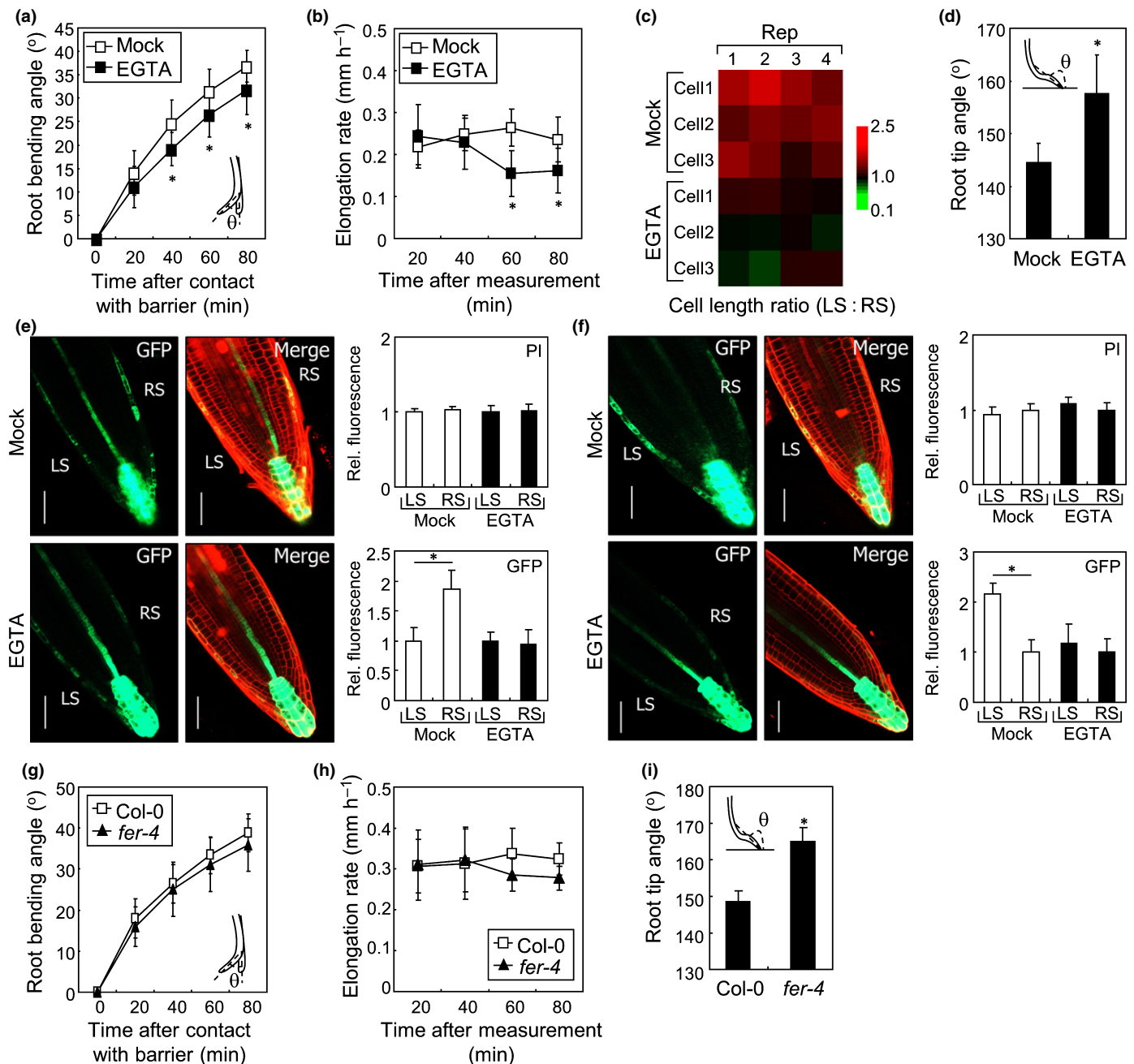


**Fig. 6**  $\text{Ca}^{2+}$  signalling affects root–obstacle avoidance. Here, 5-d-old *Arabidopsis* seedlings grown on MS agar plates were used for the assays. Eight replicates were averaged and statistically analysed using Student's *t*-test (\*,  $P < 0.01$ ). Whiskers,  $\pm$ SD. LS and RS indicate left and right side of the roots, respectively. (a) Effect of EGTA on the first bending during obstacle avoidance. Col-0 seedlings were transferred to MS agar plates containing 2 mM EGTA before assays. Bending angles of the roots were measured as described in Fig. 1(c). (b) Effect of EGTA on root elongation rate. Col-0 seedlings were treated as described in (a). Root elongation rate was measured before contact with the barrier. (c) Cell length ratio in EGTA-treated roots during the first bending. Col-0 seedlings were treated as described in (a). Cell lengths were measured as described in Fig. 2(d). Heat map bar, cell length ( $\log_2$  value). (d) Effect of EGTA on the second bending during obstacle avoidance. Col-0 seedlings were treated as described in (a). Bending angles of the roots were measured as described in Fig. 2(g). (e, f) Auxin responses in the roots after EGTA treatment. *DR5rev::GFP* seedlings were subjected to 2 mM EGTA treatment. GFP and PI fluorescence during the first (e) and the second bending (f) were measured as described in Fig. 3(b,c), respectively. Bars, 50  $\mu\text{m}$ . Fluorescence intensities were measured using IMAGEJ software. Four replicates were averaged. (g) First bending of *fer-4* roots during obstacle avoidance. Bending angles of the roots were measured as described in Fig. 1(c). (h) Root elongation rate of *fer-4* roots. Root elongation rate was measured before contact with the barrier. (i) Second bending of *fer-4* roots during obstacle avoidance. Bending angles of the roots were measured as described in Fig. 2(g).

of the bent roots. The asymmetrical auxin response would accelerate first bending. After the roots bent away from the obstacle, PIN and other auxin transporters promoted a gravity-oriented

second bending. Roots then grew parallel to the barrier keeping a step-like architecture until they found the edge of the obstacle. However, our data suggested that roots can also avoid obstacles

passively in the absence of auxin action, because auxin receptor mutants exhibited delayed, but clear, root bending after contact with a barrier (Fig. 2a,b). Therefore, the role of auxin during obstacle avoidance is in the acceleration of root bending. The next question is the physiological meaning behind rapid root bending during obstacle avoidance. To find nutrients and anchor themselves, roots should grow down into the deep soils. If plants grow in high density, finding useful resources faster than competitors is important for survival, particularly in environments with limited availability of resources. In addition, rapid anchoring is critical for plant survival under windy and harsh conditions. It is therefore possible that plants have developed the strategy of auxin-mediated rapid root movement to efficiently avoid obstacles for their survival.

### Relationship between obstacle avoidance and gravitropism

During obstacle avoidance, the second bending occurs after the roots bend away from the obstacle. The purpose of the second bending is to monitor the surface of the obstacle until the roots find the edge. Our data showed that the second bending was highly similar to root gravitropism. Auxin accumulated in the gravity-oriented cells by polar auxin transport. PINs mediated second bending (Figs 5d, S6), which is involved in gravitropism (Abas *et al.*, 2006; Rakusová *et al.*, 2011). EGTA inhibited both second bending and root gravitropism (Fig. 6d; Sinclair & Trewavas, 1997; Takahashi *et al.*, 2009). Therefore, our data cannot differentiate between second bending and gravitropism. A previous study on FER function suggested a difference between obstacle-mediated second bending and gravitropism (Shih *et al.*, 2014). The authors showed that *fer* mutants exhibited impaired second bending, but that the gravitropic responses of *fer* mutants and wild-type plants were similar (Shih *et al.*, 2014). This means that second bending and gravitropism are regulated by different molecular mechanisms. However, other recent studies have reported that *fer* mutants exhibited delayed root gravitropism (Barbez *et al.*, 2017; Dong *et al.*, 2019). Therefore, it is still unclear whether impaired second bending in *fer* mutants is due to a malfunction in gravitropism or due to other reasons. Careful analysis of FER function is required to identify the relationship between the second bending and gravitropism.

After the second bending, roots grow parallel to the obstacle. When they find the edge of the barrier, roots immediately start to grow in the direction of gravity (Massa & Gilroy, 2003). These observations indicated that gravity cannot trigger asymmetrical cell growth while the roots interact with the obstacle. Therefore, there are complicated interactions between obstacle avoidance and gravitropism. Further studies on the regulatory mechanisms of auxin transporters in relation to both obstacle avoidance and gravitropism will be helpful to identify strategies of roots during root–obstacle interaction.

### Role of $\text{Ca}^{2+}$ during root–obstacle avoidance

$\text{Ca}^{2+}$  signalling is closely involved in plant responses to mechanical stimuli. A transient increase in cytosolic  $\text{Ca}^{2+}$  level is observed

when roots undergo bending (Shih *et al.*, 2014). During the first bending, a biphasic  $\text{Ca}^{2+}$  peak is observed on the convex side of the roots (Monshausen *et al.*, 2009). The second  $\text{Ca}^{2+}$  peak is diminished in *fer* mutants (Shih *et al.*, 2014), indicating that FER is required for the second  $\text{Ca}^{2+}$  response but not for the initial  $\text{Ca}^{2+}$  response. In our study, *fer-4* roots only exhibited different responses in the second bending during obstacle avoidance (Fig. 6g,i). These results suggested that among the biphasic  $\text{Ca}^{2+}$  responses, the initial  $\text{Ca}^{2+}$  response is related to the first bending, while the late  $\text{Ca}^{2+}$  response is involved in the second bending. However, the relationship between the  $\text{Ca}^{2+}$  responses and the second bending is still unclear, because *fer* mutants exhibit pleiotropic phenotypes including delayed gravitropism (Barbez *et al.*, 2017; Dong *et al.*, 2019). Systematic analysis of  $\text{Ca}^{2+}$  responses during obstacle avoidance is necessary to identify the clear role of  $\text{Ca}^{2+}$  signalling during obstacle avoidance.

While we found that  $\text{Ca}^{2+}$  signalling is involved in root–obstacle avoidance and auxin distribution, it is still unknown how  $\text{Ca}^{2+}$  affects auxin accumulation. Our data showed that PINs are closely related to the obstacle avoidance, but blocking  $\text{Ca}^{2+}$  signalling by EGTA treatment did not affect *PIN2* gene expression (Fig. S8). As PIN proteins are highly dynamic during root tropism (Friml *et al.*, 2002; Abas *et al.*, 2006; Galván-Ampudia *et al.*, 2013), it is possible that PIN proteins are regulated by  $\text{Ca}^{2+}$  signalling. Careful analysis of PIN protein dynamics during obstacle avoidance will be necessary to identify molecular mechanisms on root movement.

### Possible role of auxin during thigmotropism

Auxin is required for tropic movement of the plants including phototropism, gravitropism, and halotropism (Abas *et al.*, 2006; Wan *et al.*, 2012; Galván-Ampudia *et al.*, 2013). Our data proposed that auxin is also involved in root bending during obstacle avoidance. Movement of the roots when they meet obstacles is highly similar to the thigmotropism observed in vine stems. Unlike roots, vine stems bend toward obstacles and twine up them to support themselves. As auxin-mediated asymmetrical cell growth is a general mechanism for plant tropic responses, our work would be applicable in identifying molecular mechanisms of thigmotropism observed in vine stems. Auxin inhibits cell elongation in the roots but it promotes cell growth in the shoots (Ottenschläger *et al.*, 2003; Swarup *et al.*, 2007; Ding *et al.*, 2011). It is therefore possible that auxin transporter-mediated polar auxin transport is activated when vine stems meet obstacles. Further studies on vine stems using auxin reporters will be helpful to uncover underlying mechanisms of thigmotropism.

### Explorative behaviour of roots

Plant roots exhibit distinct movement to explore the surrounding space. In addition to the thigmotropic movement described in this work, light-grown roots circumnutate in the empty space (Yokawa & Baluška, 2018). This behaviour may be necessary to escape from unfavourable conditions. Notably, spiral movement

of maize roots is largely reduced in the dark (Yokawa & Baluška, 2018). These observations suggest that root movement is closely related to other environmental signals. Negative phototropism of roots also shows that roots sense light (Burbach *et al.*, 2012; Yokawa *et al.*, 2013; Suzuki *et al.*, 2016). It is therefore possible that obstacle avoidance is also affected by surrounding light conditions. Analysis of root thigmotropic behaviour under different light conditions would be a good approach to uncover these questions.






## Acknowledgements

We thank Hyang Ran Yoon for managing the confocal microscopy. We also thank Martin van Rongen and Ottoline Leyser for providing the *pin3 pin4 pin7* triple mutant seeds. This work was supported by the Basic Research Program provided by the National Research Foundation of Korea (NRF-2019R1C1C1002045) and the KRIBB Research Initiative Program (KGM5371911).

## Author contributions

H-JL conceived, designed and performed the experiments. H-SK and JHJ provided experimental tools and equipment. H-JL prepared the manuscript with the contributions of H-SK, JMP and HSC.

## ORCID

Hye Sun Cho  <https://orcid.org/0000-0003-0469-7186>  
Jae Heung Jeon  <https://orcid.org/0000-0002-4503-5659>  
Hyun-Soon Kim  <https://orcid.org/0000-0002-9054-0689>  
Hyo-Jun Lee  <https://orcid.org/0000-0002-0690-7522>  
Jeong Mee Park  <https://orcid.org/0000-0002-3344-7875>

## References

- Abas L, Benjamins R, Malenica N, Paciorek T, Wiśniewska J, Moulinier-Anzola JC, Sieberer T, Friml J, Luschig C. 2006. Intracellular trafficking and proteolysis of the *Arabidopsis* auxin-efflux facilitator PIN2 are involved in root gravitropism. *Nature Cell Biology* 8: 249–256.
- Barbez E, Dünser K, Gaidora A, Lendl T, Busch W. 2017. Auxin steers root cell expansion via apoplastic pH regulation in *Arabidopsis thaliana*. *Proceedings of the National Academy of Sciences, USA* 114: E4884–E4893.
- Blilou I, Xu J, Wildwater M, Willemsen V, Paponov I, Friml J, Heidstra R, Aida M, Palme K, Scheres B. 2005. The PIN auxin efflux facilitator network controls growth and patterning in *Arabidopsis* roots. *Nature* 433: 39–44.
- Braam J. 2005. In touch: plant responses to mechanical stimuli. *New Phytologist* 165: 373–389.
- Braam J, Davis RW. 1990. Rain-, wind-, and touch-induced expression of calmodulin and calmodulin-related genes in *Arabidopsis*. *Cell* 60: 357–364.
- Brunoud G, Wells DM, Oliva M, Larrieu A, Mirabet V, Burrow AH, Beeckman T, Kepinski S, Traas J, Bennett MJ *et al.* 2012. A novel sensor to map auxin response and distribution at high spatio-temporal resolution. *Nature* 482: 103–106.
- Burbach C, Markus K, Zhang Y, Schlicht M, Baluška F. 2012. Photophobic behavior of maize roots. *Plant Signaling & Behavior* 7: 874–878.
- Cohen B. 2006. Urbanization in developing countries: current trends, future projections, and key challenges for sustainability. *Technology in Society* 28: 63–80.
- Dharmasiri N, Dharmasiri S, Estelle M. 2005a. The F-box protein TIR1 is an auxin receptor. *Nature* 435: 441–445.
- Dharmasiri N, Dharmasiri S, Weijers D, Lechner E, Yamada M, Hobbie L, Ehrismann JS, Jürgens G, Estelle M. 2005b. Plant development is regulated by a family of auxin receptor F box proteins. *Developmental Cell* 9: 109–119.
- Ding Z, Galván-Ampudia CS, Demarsy E, Łangowski Ł, Kleine-Vehn J, Fan Y, Morita MT, Tasaka M, Fankhauser C, Offringa R *et al.* 2011. Light-mediated polarization of the PIN3 auxin transporter for the phototropic response in *Arabidopsis*. *Nature Cell Biology* 13: 447–452.
- Dong Q, Zhang Z, Liu Y, Tao LZ, Liu H. 2019. FERONIA regulates auxin-mediated lateral root development and primary root gravitropism. *FEBS Letters* 593: 97–106.
- Fendrych M, Leung J, Friml J. 2016. TIR1/AFB-Aux/IAA auxin perception mediates rapid cell wall acidification and growth of *Arabidopsis* hypocotyls. *eLife* 5: e19048.
- Friml J, Wiśniewska J, Benková E, Mendgen K, Palme K. 2002. Lateral relocation of auxin efflux regulator PIN3 mediates tropism in *Arabidopsis*. *Nature* 415: 806–809.
- Galván-Ampudia CS, Julkowska MM, Darwish E, Gandullo J, Korver RA, Brunoud G, Haring MA, Munnik T, Vernoux T, Testerink C. 2013. Halotropism is a response of plant roots to avoid a saline environment. *Current Biology* 23: 2044–2050.
- Godfray HCJ, Beddington JR, Crute IR, Haddad L, Lawrence D, Muir JF, Pretty J, Robinson S, Thomas SM, Toulmin C. 2010. Food security: the challenge of feeding 9 billion people. *Science* 327: 812–818.
- He W, Brumos J, Li H, Ji Y, Ke M, Gong X, Zeng Q, Li W, Zhang X, An F *et al.* 2011. A small-molecule screen identifies L-kynurenine as a competitive inhibitor of TAA1/TAR activity in ethylene-directed auxin biosynthesis and root growth in *Arabidopsis*. *Plant Cell* 23: 3944–3960.
- Jensen GS, Fal K, Hamant O, Haswell ES. 2017. The RNA polymerase-associated factor 1 complex is required for plant touch responses. *Journal of Experimental Botany* 68: 499–511.
- Lambin EF, Meyfroidt P. 2011. Global land use change, economic globalization, and the looming land scarcity. *Proceedings of the National Academy of Sciences, USA* 108: 3465–3472.
- Lewis DR, Miller ND, Splitt BL, Wu G, Spalding EP. 2007. Separating the roles of acropetal and basipetal auxin transport on gravitropism with mutations in two *Arabidopsis* multidrug resistance-like ABC transporter genes. *Plant Cell* 19: 1838–1850.
- Lobell DB, Schlenker W, Costa-Roberts J. 2011. Climate trends and global crop production since 1980. *Science* 333: 616–620.
- Long H, Tang G, Li X, Heilig GK. 2007. Socio-economic driving forces of land-use change in Kunshan, the Yangtze River Delta economic area of China. *Journal of Environmental Management* 83: 351–364.
- Ma Y, Zhao Y, Berkowitz GA. 2017. Intracellular  $Ca^{2+}$  is important for flagellin-triggered defense in *Arabidopsis* and involves inositol polyphosphate signaling. *Journal of Experimental Botany* 68: 3617–3628.
- Massa GD, Gilroy S. 2003. Touch modulates gravity sensing to regulate the growth of primary roots of *Arabidopsis thaliana*. *The Plant Journal* 33: 435–445.
- Monshausen GB, Bibikova TN, Weissenel MH, Gilroy S. 2009.  $Ca^{2+}$  regulates reactive oxygen species production and pH during mechanosensing in *Arabidopsis* roots. *Plant Cell* 21: 2341–2356.
- Nakagawa Y, Katagiri T, Shinozaki K, Qi Z, Tatsumi H, Furuichi T, Kishigami A, Sokabe M, Kojima I, Sato S *et al.* 2007. *Arabidopsis* plasma membrane protein crucial for  $Ca^{2+}$  influx and touch sensing in roots. *Proceedings of the National Academy of Sciences, USA* 104: 3639–3644.
- Nishimura T, Hayashi K, Suzuki H, Gyohda A, Takaoka C, Sakaguchi Y, Matsumoto S, Kasahara H, Sakai T, Kato J *et al.* 2014. Yucasin is a potent inhibitor of YUCCA, a key enzyme in auxin biosynthesis. *The Plant Journal* 77: 352–366.
- Ottenschlager I, Wolff P, Wolvertson C, Bhalerao RP, Sandberg G, Ishikawa H, Evans M, Palme K. 2003. Gravity-regulated differential auxin transport from columella to lateral root cap cells. *Proceedings of the National Academy of Sciences, USA* 100: 2987–2991.
- Peng S, Huang J, Sheehy JE, Laza RC, Visperas RM, Zhong X, Centeno GS, Khush GS, Cassman KG. 2004. Rice yields decline with higher night



- temperature from global warming. *Proceedings of the National Academy of Sciences, USA* 101: 9971–9975.
- Rakusová H, Gallego-Bartolomé J, Vanstraelen M, Robert HS, Alabadi D, Blázquez MA, Benková E, Friml J. 2011. Polarization of PIN3-dependent auxin transport for hypocotyl gravitropic response in *Arabidopsis thaliana*. *The Plant Journal* 67: 817–826.
- Sabatini S, Beis D, Wolkenfelt H, Murfett J, Guilfoyle T, Malamy J, Benfey P, Leyser O, Bechtold N, Weisbeek P *et al.* 1999. An auxin-dependent distal organizer of pattern and polarity in the *Arabidopsis* root. *Cell* 99: 463–472.
- Schlenker W, Lobell DB. 2010. Robust negative impacts of climate change on African agriculture. *Environmental Research Letters* 5: 014010.
- Shih HW, Miller ND, Dai C, Spalding EP, Monshausen GB. 2014. The receptor-like kinase FERONIA is required for mechanical signal transduction in *Arabidopsis* seedlings. *Current Biology* 24: 1887–1892.
- Sinclair W, Trewavas AJ. 1997. Calcium in gravitropism. A re-examination. *Planta* 203: S85–S90.
- Suzuki H, Yokawa K, Nakano S, Yoshida Y, Fabrisin I, Okamoto T, Baluška F, Koshida T. 2016. Root cap-dependent gravitropic U-turn of maize root requires light-induced auxin biosynthesis via the YUC pathway in the root apex. *Journal of Experimental Botany* 67: 4581–4591.
- Swarup R, Perry P, Hagenbeek D, Van Der Straeten D, Beemster GT, Sandberg G, Bhalerao R, Ljung K, Bennett MJ. 2007. Ethylene upregulates auxin biosynthesis in *Arabidopsis* seedlings to enhance inhibition of root cell elongation. *Plant Cell* 19: 2186–2196.
- Takahashi H, Miyazawa Y, Fujii N. 2009. Hormonal interactions during root tropic growth: hydrotropism versus gravitropism. *Plant Molecular Biology* 69: 489–502.
- Tanaka K, Gilroy S, Jones AM, Stacey G. 2010. Extracellular ATP signaling in plants. *Trends in Cell Biology* 20: 601–608.
- Tilman D, Balzer C, Hill J, Belfort BL. 2011. Global food demand and the sustainable intensification of agriculture. *Proceedings of the National Academy of Sciences, USA* 108: 20260–20264.
- Waldie T, Leyser O. 2018. Cytokinin targets auxin transport to promote shoot branching. *Plant Physiology* 177: 803–818.
- Wan Y, Jasik J, Wang L, Hao H, Volkmann D, Menzel D, Mancuso S, Baluška F, Lin J. 2012. The signal transducer NPH3 integrates the Phototropin1 photosensor with PIN2-based polar auxin transport in *Arabidopsis* root phototropism. *Plant Cell* 24: 551–565.
- Weerasinghe RR, Swanson SJ, Okada SF, Garrett MB, Kim SY, Stacey G, Boucher RC, Gilroy S, Jones AM. 2009. Touch induces ATP release in *Arabidopsis* roots that is modulated by the heterotrimeric G-protein complex. *FEBS Letters* 583: 2521–2526.
- Yokawa K, Baluška F. 2018. Sense of space: tactile sense for exploratory behavior of roots. *Communicative & Integrative Biology* 11: 1–5.
- Yokawa K, Kagenishi T, Baluška F. 2013. Root photomorphogenesis in laboratory-maintained *Arabidopsis* seedlings. *Trends in Plant Science* 18: 117–119.
- Zhang X, Mou Z. 2009. Extracellular pyridine nucleotides induce *PR* gene expression and disease resistance in *Arabidopsis*. *The Plant Journal* 57: 302–312.

## Supporting Information

Additional Supporting Information may be found online in the Supporting Information section at the end of the article.

**Fig. S1** Root phenotype of *tir1 afb1 afb2 afb3* quadruple mutants.

**Fig. S2** An example of root cell length measurement during first bending.

**Fig. S3** DII-VENUS fluorescence during root–obstacle avoidance.

**Fig. S4** Effect of L-Kyn on root–obstacle avoidance.

**Fig. S5** Obstacle avoidance of *eir1-1* roots.

**Fig. S6** The *pin3 pin4 pin7* triple mutants exhibit altered obstacle avoidance.

**Fig. S7** Obstacle avoidance of *aux1-7* mutants.

**Fig. S8** Expression of *PIN2* gene during first bending.

Please note: Wiley Blackwell are not responsible for the content or functionality of any Supporting Information supplied by the authors. Any queries (other than missing material) should be directed to the *New Phytologist* Central Office.